J. Chem. Sci. (2020) 132:141
https://doi.org/10.1007/s12039-020-01843-9

REGULAR ARTICLE

Synthesis, characterization, DNA-binding and biological studies of novel titanium (IV) complexes

RAJ KAUSHAL[a,*], ARCHANA THAKUR[a], ASTHA BHATIA[b], SAROJ ARORA[b] and KIRAN NEHRA[c]

[a]Department of Chemistry, National Institute of Technology, Hamirpur, Himachal Pradesh 177 005, India
[b]Department of Botanical and Environmental Sciences, Guru Nanak Dev University, Amritsar, Punjab 143005, India
[c]Department of Biotechnology, Deenbandhu Chhotu Ram University of Science and Technology, Murthal (Sonepat), Haryana 131039, India
E-mail: kaushalraj384@gmail.com; thakurarchana009@gmail.com; asthabhatia66@gmail.com; sarojarora.gndu@gmail.com; nehrakiran@gmail.com

MS received 25 June 2020; revised 10 August 2020; accepted 10 August 2020

Abstract. A series of novel binuclear titanium (IV) complexes, $[Ti(sal)L^{I–V}(OBu)(\mu\text{-}OBu)]_2$, was synthesized by the reaction of salicylic acid (H_2sal) and substituted indoles (L^I = Tryptophol, L^{II} = 5-Methoxyindole, L^{III} = Indole-5-Carboxaldehyde, L^{IV} = 5-Cyanoindole, L^V = 6-Nitroindole) with titanium(IV) tetrabutoxide in predetermined molar ratios under stirring and refluxing conditions in THF solvent. The chemical structure of synthesized complexes was found to be binuclear based on the FTIR, ^{1}H (proton) NMR and ESI-Mass (Electron-spray ionization) spectroscopic data. Each titanium metal was surrounded by two bridged butoxy groups and one terminal butoxy group along with bidentate salicylic acid and coordinated substituted indoles. These complexes were investigated for antioxidant potential using DPPH (2,2-diphenyl-1-picrylhydrazyl) assay where they exhibited moderate to good antioxidant activity. Gel electrophoresis method was employed to study the ct-DNA (calf thymus DNA) cleavage efficiency of complexes using an agarose gel. Antimicrobial results stated that most of the complexes were ineffective against selected bacterial and fungal strains. Complexes were investigated for anticancer activity against two selected cancerous cell lines (L6 and L929). From MTT (3-(4,5-dimethylthiazol-2-yl)-2,5-diphenyl tetrazolium bromide) assay, it has been inferred that complexes **1** and **2** have better anticancer properties than their respective indoles. The DNA binding study of synthesized complexes studied in order to check their efficacy to hinder DNA replication/transcription using electronic absorption and fluorescence spectroscopy revealed them as electrostatic/groove binder. The synthesized complexes were also evaluated for antidiabetic properties using alpha-amylase inhibition assay and complex **5** possessed better alpha-amylase inhibition activity than other complexes.

Keywords. DNA cleavage; Indole; MTT assay; Salicylic acid; Titanium butoxide.

1. Introduction

In transition metal chemistry, alkoxides were treated as ancillary ligands forming ionic bonds with first-row transition metals.[1] They exhibit poor σ-donating ability but the existence of oxygen atom bearing three lone pair of electrons made them better π-donating ligands.[2] Metal alkoxides being very reactive species generally used to synthesize metal oxides. Their rate of hydrolysis is generally high which can be controlled by reacting them with nucleophilic ligands.[3] Mehrotra *et al.,* and Sanchez *et al.,* studied the metal alkoxide chemistry in detail and reported that molecular complexity of metal in metal alkoxide, M(OR) (M = Ti, Zn, Hf, Th) is directly proportional to its atomic size and inversely proportional to the bulkiness of alkoxy group.[4, 5] In the literature survey, the titanium alkoxide had large industrial applications. Indole derivatives

*For correspondence

Electronic supplementary material: The online version of this article (https://doi.org/10.1007/s12039-020-01843-9) contains supplementary material, which is available to authorized users.

Published online: 22 October 2020

attracted our attention because of their unique property to mimic the structure of peptides and reversible binding ability with enzymes,[6–9] thereby creating opportunities to invent novel drugs with separate modes of action. A large number of molecules having the indole nucleus got FDA approval and are used in drug therapies. Natural and synthetic derivatives of indole moiety possess antibacterial, anticancer, antioxidant, etc., properties.[10] Also, indole complexes with different metals (copper, cobalt, nickel, zinc) show a good range of pharmaceutical activities.[11] Despite potential applications of titanium alkoxide and substituted indoles, limited studies on titanium alkoxide complexes and their indole derivatives as pharmacological agents were carried out.

In the present chapter, we herein report the synthesis and characterization of mixed ligand binuclear titanium (IV) butoxide. Synthesized complexes were investigated for their interactions with ct-DNA in order to enhance the specificity of target and stability of recognition with respect to DNA. Most of the chemotherapeutic anticancer agents are characterized as DNA-binding drugs because they have the potential to interfere with DNA transcription and replication. These drug-DNA interactions can provide further knowledge of the interaction mechanism between DNA and anticancer drugs. The anticancer drug binds with DNA in three different ways. In the first method, the anticancer drug controls transcription and polymerases by interacting with such proteins that bind straight with DNA. In the second method, the formation of DNA-RNA hybrids takes place through RNA binding to double helices of DNA, thus obstructing transcriptional activity. In the third method, non-covalent interactions of small ligands with DNA structure include a groove or intercalating binders.[12, 13] The synthesized drugs have various potential applications including cancer and other which created significant interest in their discovery and characterization.[14] Thus the knowledge of the mechanism of drug-DNA interaction can help in the design of new DNA-targeted drugs. Further antioxidant, antibacterial, antifungal and alpha-amylase inhibition activities were studied. The anticancer activity of ligands and synthesized complexes were evaluated against L6 skeletal muscle cell line and L929 cancer cell line.

2. Materials and methods

Titanium butoxide, salicylic acid, substituted indoles, ct-DNA were obtained from Sigma Aldrich. Tetrahydrofuran, ethanol purchased from Merck were dried using standard procedure before use. ^{1}H and ^{13}C NMR spectra of complexes in d_6-DMSO were recorded with 400 MHz Bruker Avance spectrometer. Evaluation of infra-red, UV-visible spectra of complexes were done on PerkinElmer 1600 spectrometer using KBr discs (400–4000 cm^{-1}) and PerkinElmer Lambda 750, respectively.

2.1 *Preparation of [Ti(sal)L^{I}(OBu)(μ-OBu)]$_2$ (**1**)*

Salicylic acid (0.5 mM, 0.081 g) was dissolved in 30 mL of THF. Titanium butoxide (0.5 mM, 0.200 g) was added to the resulting solution with continuous stirring. The colour of the mixture changes to yellow and then to orange on complete addition. Then the reaction mixture was refluxed till its colour got stabilized to yellow. To this yellow coloured solution, tryptophol (0.5 mM, 0.095 g) was added with continuous stirring. No change in colour was observed during and after addition of ligand (L^{I}). The reaction solution was then refluxed for about 15 h. The overall reaction was performed under inert nitrogen atmosphere. TLC technique was used for monitoring of reaction progress. Yellow coloured precipitates so obtained were filtered and dried on calcium chloride; Yellow solid, yield (75%); decomposition temperature > 290 °C; IR (KBr) ν_{max} 3364, 1602, 1377, 1250, 1140, 1123, 1034, 548, 524, 420 cm^{-1}; ^{1}H NMR (d6 DMSO, 400 MHz,) δ (ppm): 0.87, 1.28–1.39, 3.42 (terminal butoxy group); 0.93, 1.37–1.41, 4.32 (bridged butoxy group); 6.94–7.95 (aromatic protons); 8.19 (N–H proton).

A similar method was chosen for the synthesis of complexes 2, 3, 4 and 5.

2.2 *Preparation of [Ti(sal)L^{II}(OBu)(μ-OBu)]$_2$ (**2**)*

Yellow solid, yield (72%); decomposition temperature > 290 °C; IR (KBr) ν_{max} 3268, 1601, 1392, 1247, 1145, 1102, 1034, 543, 530, 412 cm^{-1}; ^{1}H NMR (d6 DMSO, 400 MHz,) δ (ppm): 0.86, 1.23–1.38, 3.18 (terminal butoxy group); 0.95, 1.36–1.42, 4.30 (bridged butoxy group); 6.58–7.74 (aromatic protons); 10.42 (N–H proton).

2.3 *Preparation of [Ti(sal)L^{III}(OBu)(μ-OBu)]$_2$ (**3**)*

Red solid, yield (78%); decomposition temperature > 300 °C; IR (KBr) ν_{max} 3388, 1670, 1603, 1357, 1236, 1125, 1093, 1032, 547, 532, 427 cm^{-1}; ^{1}H NMR (d6 DMSO, 400 MHz,) δ (ppm): 0.84, 1.20–1.36, 3.35 (terminal butoxy group); 0.88, 1.35–1.45, 4.25 (bridged butoxy group); 6.63–7.90 (aromatic protons), 9.70 (N–H proton), 11.13 (C–H aldehydic proton).

2.4 *Preparation of [Ti(sal)L^{IV}(OBu)(μ-OBu)]$_2$ (**4**)*

Yellow solid, yield (70%); decomposition temperature > 290 °C; IR (KBr) ν_{max} 3309, 1602, 1393, 1255,

1144, 1087, 1029, 559, 530, 423 cm^{-1}; ^1H NMR (d6 DMSO, 400 MHz,) δ (ppm): 0.85, 1.30–1.39, 3.35 (terminal butoxy group); 0.94, 1.38–1.42, 4.35 (bridged butoxide group); 6.59–7.81 (aromatic protons), 10.59 (N–H proton).

2.5 *Preparation of $[Ti(sal)L^V(OBu)(\mu\text{-}OBu)]_2$ (**5**)*

Yellow solid, yield (80%); decomposition temperature > 290 °C; IR (KBr) ν_{max} 3203, 1601, 1395, 1246, 1145, 1101, 1034, 555, 532, 420 cm^{-1}; ^1H NMR (d6 DMSO, 400 MHz,) δ (ppm): 0.86, 1.14–1.35, 3.34 (terminal butoxy group); 0.98, 1.34–1.44, 4.38 (bridged butoxide group), 6.55–7.79 (aromatic protons), 10.78 (N–H proton).

2.6 *DNA-binding studies using UV-visible absorption spectroscopy*

The ct-DNA binding experiment was conducted in 5 mM TrisHCl and 50 mM NaCl buffer at pH 7.2. For DNA interaction studies, titanium complexes were dissolved in a little amount of DMSO for complete solubility and then diluted with buffer. The solution of ct-DNA was prepared in doubly-distilled water and kept overnight for complete dissolution at 4 °C. In order to check the ct-DNA interactions with metal complexes, an increasing amount of DNA was added to the fixed concentration of titanium complex. The spectra of each complex- DNA solution was recorded after the incubation time of 10 min. From spectral titration data, the intrinsic binding constant (known as K_b) was determined for metal complexes using the following equation[15]:

$$\frac{A_0}{A - A_0} = \frac{\varepsilon_G}{\varepsilon_{H-G} - \varepsilon_G} + \left(\frac{\varepsilon_G}{\varepsilon_{H-G} - \varepsilon_G}\right) \times \frac{1}{K[DNA]}$$

where A_0 and A correspond to the absorbance of DNA alone and DNA-complex, respectively; K denotes binding constant and ε_G and ε_{H-G} are the absorption coefficients of drug and drug-DNA complex, respectively.

2.7 *DNA-binding study using fluorescence spectroscopy*

The fluorescence spectra of fixed concentration of synthesized titanium complexes in TrisHCl/NaCl (5 mM/50 mM) buffer (pH 7.2) was measured in the absence and presence of the increasing amount of ct-DNA. The excitation and emission wavelength were at 320 and 415 nm, respectively. The fluorescence spectra of all complexes were recorded from 350 to 550 nm.

2.8 *Antioxidant studies*

Spectrophotometric method was used to conduct the radical scavenging activity of titanium complexes using DPPH (1,1-diphenyl-2,2-picrylhydrazyl) at 517 nm.[16] To the different concentration of titanium complexes (10, 50, 80, 100 and 200 μM) and ascorbic acid (standard), 0.1 mM methanolic solution of DPPH was added. Before taking the absorbance at 517 nm, the samples were incubated for half an hour. The following equation 2 gave the percentage free radical scavenging activity:

$$\% \text{ Scavenging Activity} = [(A_0 - A_s)/A_0] \times 100$$

where A_0 and A_s correspond to the absorbance of the control (DPPH) and sample, respectively.

2.9 *DNA cleavage activity*

The DNA cleavage efficacy of titanium complexes was examined using ct-DNA using agarose gel electrophoresis technique. 1% agarose gel made by the addition of 100 mL TAE buffer (1X) to 1 g agarose was boiled till complete dissolution and was allowed to solidify in the gel cassette after attaining 55 °C temperature. The mixture of ct-DNA (150 μM) with H_2O_2 (40 μM) and complexes (1–5) (200 μM) was incubated at 37 °C for 1 h. Loading of samples in the electrophoresis chamber full of TAE buffer was done by mixing DNA samples with bromophenol blue as dye in 1:1 ratio. Electrophoresis was performed at a constant voltage of 50 V for 45 min. Gel was stained in ethidium bromide solution (1 μg/mL) for 10 min and destained for the same time interval in double-distilled water. Bands were observed using UV light in the darkroom.

2.10 *Antibacterial and antifungal studies*

Antimicrobial activity was accomplished by agar well diffusion method.[17] Synthesized metal complexes were screened for in-vitro antibacterial activity against *P. aeruginosa* (***MTCC-3542***), *E. coli* (***MTCC-9721***), *L. monocytogenes* (***MTCC-675***), *B. cereus* (***MTCC-1272***), *S. aureus* (***MTCC-11949***) and *S. flexneri* (***MTCC-1457***) using nutrient agar as media. Briefly, the heated nutrient agar was kept at 45 °C and poured into petri plates for solidification. Test samples (3 mg/mL) were prepared in DMSO. Then the wells punched with cup-borer were filled with sample solution (20 μL) and bacterial strains (100 μL). Each plate was incubated for 24 h at 37 °C to get the inhibition zone of diameter. Results were compared with a standard drug tetracycline kept under identical conditions as the test samples.

Antifungal activity of titanium complexes (1–5) were screened against *B. cinerea, A. niger, A. alternate* and *P. expansum* using agar well method on potato dextrose media. Similar procedure as described above was adopted with incubation time for 72 h at 37 °C. Results of the zone of inhibition were compared against fluconazole (standard). Zone of inhibition for DMSO (negative control) was found negligible.

2.11 *Anticancer study*

An *in-vitro* preliminary test was conducted on immortalized cell line L6 and cancer cell line L929 using MTT (3-(4,5-dimethylthiazol-2-yl)-2,5-diphenyl tetrazolium bromide) assay on 96-well plate.[18] Briefly, the complexes of different concentrations were prepared by dissolving the appropriate amount of complex in a minimum amount of DMSO and diluted to the desired concentration. The increasing concentration of complexes was added to the suspension (5×10^3 cells) of L929 and L6 cells. Post-treatment involved the addition of MTT (100 µL) into each well at 37 °C for 4 h. After incubation, the resulting solution was subjected for aspiration followed by the suspension of MTT formazan crystals in 100 µL DMSO. The optical density was recorded using BioTek Synergy HT ELISA reader at 570 nm. Cytotoxicity was measured using the following formula:

$$\% \text{ Inhibition} = [(A_c - A_s)/A_c] \times 100$$

where A_c - absorbance of the control, A_s - absorbance of the sample. IC_{50} was calculated using a regression equation obtained from experimental data.

2.12 *α-amylase inhibition activity*

The inhibitory activities of titanium complexes against α-amylase were investigated with some modifications.[19] Each 10 µL of 20 U/mL α-amylase, titanium complexes of different concentrations with 0.01 M phosphate buffer (pH 7.2) was mixed and incubated at 37 °C for 30 min. After incubation, 100 µL of 1% starch solution (w/v) was added and further incubated for 20 min. 100 µL of HCl (1 M) was added to each dilution to get the reaction terminated. The absorbance of the reaction mixture was followed after the addition of 200 µL of 1% iodine solution and 1.6 mL water. The (%) inhibitory activity was obtained from the following equation:

$$\% \text{ Inhibition Activity} = \frac{A_s - A_b}{A_c - A_b} \times 100$$

where A_s is the absorbance of the sample, A_b is the absorbance of blank (without starch and sample) and A_c is the absorbance of the control (without enzyme and sample).

3. Results and discussion

The reaction of titanium butoxide with salicylic acid (H_2L) was carried out under stirring and refluxing in 1:1 molar ratio in THF at room temperature till its colour stability. The respective substituted indoles ($L^{I–V}$) were added to the above mixture in 1:1 molar ratio using THF as a solvent. The reaction mixture was refluxed till the completion. Progress of the reaction was monitored by TLC method. Excess solvent was removed by vacuum distillation and products were obtained as shown in Scheme 1.

All synthesized mixed ligand titanium butoxide complexes were coloured solids in appearance and are soluble in polar solvents like DMSO. The yield of synthesized titanium complexes (1–5) was 70–80%. Physico-analytical data is tabulated in Table 1.

3.1 *FTIR characterization*

FTIR spectral data of ligands (H_2sal, $L^{I–V}$) and complexes (1–5) has been shown in Table T1, Supplementary Information. In the FTIR spectrum of pure salicylic acid (H_2sal), the C=O (COO^-) asymmetric and symmetric carbonyl stretching vibrations were observed at 1656 and 1383 cm^{-1}, respectively. Further, the peaks appearing at frequency 1558–1609 cm^{-1} were attributed due to C=C stretching. Peaks observed at 3230 cm^{-1} and 2851 cm^{-1} were assigned due to OH and CH stretching vibrations

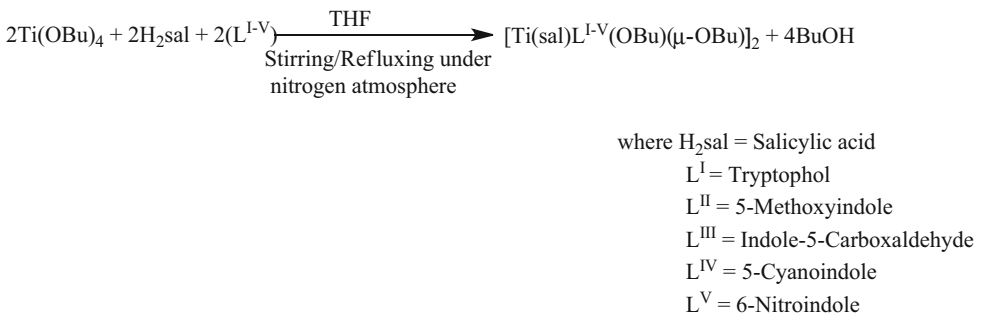

Scheme 1. Synthesis of complexes $[Ti(sal)L^{I–V}(OBu)(\mu\text{-}OBu)]_2$ (**1–5**).

Table 1. Analytical data and physical properties of mixed ligand titanium butoxide complexes, $[Ti(sal)L^{I–V}(OBu)(\mu\text{-}OBu)]_2$ (1–5)

Sl. No.	Complex	Color	Decomp. temperature (°C)	Elemental Analysis % calcd (found)				Yield (%)
				Ti	C	H	N	
1	$[Ti(sal)L^{I}(OBu)(\mu\text{-}OBu)]_2$ (**1**)	Yellow	> 290	9.70 (9.65)	61.16 (61.08)	3.46 (3.42)	2.85 (2.83)	75
2	$[Ti(sal)L^{II}(OBu)(\mu\text{-}OBu)]_2$ (**2**)	Yellow	> 290	9.99 (9.96)	60.44 (60.40)	6.50 (6.48)	2.93 (2.91)	72
3	$[Ti(sal)L^{III}(OBu)(\mu\text{-}OBu)]_2$ (**3**)	Red	> 300	10.03 (10.01)	60.63 (60.62)	6.10 (6.08)	2.95 (2.92)	78
4	$[Ti(sal)L^{IV}(OBu)(\mu\text{-}OBu)]_2$ (**4**)	Yellow	> 290	10.09 (10.05)	61.02 (61.00)	5.93 (5.90)	5.93 (5.92)	70
5	$[Ti(sal)L^{V}(OBu)(\mu\text{-}OBu)]_2$ (**5**)	Yellow	> 290	9.68 (9.62)	56.15 (56.12)	5.69 (5.64)	5.69 (5.66)	80

respectively. Also, the phenolic O-H bending vibration (Ph-OH) was found at 1324 cm^{-1} in pure salicylic acid (H_2sal). The phenolic (C–OH) and COO^- (C–O) stretching appeared at 1151 cm^{-1} and 1291 cm^{-1} respectively.[20] In all the complexes (**1–5**), the C=O (COO^-) asymmetric vibrations at 1602–1603 cm^{-1} with lowering of about 53–54 cm^{-1} while symmetric vibrations were assigned to the peaks in the FTIR spectra at 1346–1377 cm^{-1} with a negative shift of 6–37 cm^{-1} with respect to salicylic acid (H_2sal). The C–O (phenolic) and C–O (COO^-) stretching were observed in the region 1125–1145 and 1236–1255 cm^{-1}, respectively with significant lowering of wavenumber on complexation. These shifts in C=O (COO^-) asymmetric, symmetric and C–O stretching vibrations indicated the loss of carboxylic and phenolic hydrogen and the involvement of both carboxylic oxygen and phenolic oxygen in bonding with metal center. Also, the difference in stretching frequency ($\Delta\nu$) of COO^- asymmetric and symmetric vibrations lies in the range 249–256 cm^{-1}, suggested the involvement of unidentate carboxylic group with metal center.[21, 22] The FTIR spectra of all complexes showed bands in the region 1015–1034 cm^{-1} and 1087–1123 cm^{-1} corresponded to bridged and terminal butoxy groups, respectively.[23] The shift in N–H stretching vibrations was observed for all complexes (**1–5**). Further, the appearance of new bands in the region 400–500 cm^{-1} and 500–600 cm^{-1} signified the Ti–N and Ti–O bonding, respectively.[24]

In the FTIR spectrum of ligand (L^I), the peak appearing at 3385 cm^{-1} due to N–H group, shifted to lower wavenumber 3364 cm^{-1} after coordination with titanium ion indicated the involvement of nitrogen atom in bonding. The carboxylate (COO^-) asymmetric and symmetric stretching vibrations appeared at 1602 cm^{-1} and 1377 cm^{-1}, respectively with $\Delta\nu$ = 255 cm^{-1}, thereby assigning the involvement of unidentate COO– group in bonding with titanium ion. The disappearance of phenolic OH bending vibration peak suggested the loss of phenolic hydrogen (O–H) and lowering in the wavenumber due to C–O (phenolic) stretching vibrations suggested the formation of phenolate group in the complex **1**. The new vibrations at 1123 cm^{-1} and 1034 cm^{-1} appeared in the complex suggesting the formation of the terminal and bridged butoxy group, respectively. The new peaks at 420 cm^{-1} assigned to $\nu_{Ti–N}$ (L^I) while peaks at 524 cm^{-1}, 548 cm^{-1} were due to $\nu_{Ti–O}$ vibration modes of salicylate ion (sal).

In the FTIR spectrum of complex **2**, the N–H peak of indole shifted from 3391 cm^{-1} in pure ligand (L^{II}) to 3268 cm^{-1}. The lowering in wavenumber suggested the bonding of nitrogen with titanium ion. The asymmetric and symmetric carboxylate peaks were observed at 1601 cm^{-1} and 1352 cm^{-1}, respectively with difference $\Delta\nu$ = 249 cm^{-1} suggesting the involvement of unidentate CO_2 group in bonding with titanium ion. The peak due to phenolic OH bending vibration disappeared and there was lowering in the wavenumber due to stretching vibrations of C–O (phenolic) and COO^- (C–O) due to coordination to metal accompanied by loss of hydrogens from phenolic O–H and carboxylic. The appearance of new bands at 1102 cm^{-1} and 1034 cm^{-1} in the complex was due to the presence of two butoxy groups i.e., terminal and bridged, respectively. A new peak at 412 cm^{-1} was assigned for $\nu_{Ti–N}$ (L^{II}) while peaks at 530 cm^{-1}, 543 cm^{-1} were assigned to $\nu_{Ti–O}$ vibration modes of salicylate ion (sal).

In the FTIR spectrum of ligand (L^{III}), the peak at 3264 cm^{-1} corresponding to N–H group of indole

suffered a positive shift and appeared at 3388 cm^{-1} in the complex **3**. This indicated the participation of nitrogen atom in bonding titanium ion. The peak appeared at 1603 cm^{-1} and 1350 cm^{-1} corresponded to CO_2 asymmetric and symmetric stretching with the difference of 253 cm^{-1} in wavenumber. This difference in $\Delta\nu$ indicated the participation of unidentate CO_2 in bonding with titanium ion. Lowering of wavenumber due to C–O (phenolic) and COO^- (C–O) stretching vibrations was observed due to coordination to titanium metal. Bands appeared at 1093 cm^{-1} 1032 cm^{-1} signified the presence of terminal and bridged butoxy group in the complex. The new peak appeared at 427 cm^{-1} assigned to ν_{Ti-N} (L^{III}) while peaks at 532 cm^{-1}, 547 cm^{-1} assigned to ν_{Ti-O} (sal), respectively.

A broadening of the peak at 3309 cm^{-1} in complex **4** with slight positive shift after coordination due to N–H moiety of indole ligand (L^{IV}) support the involvement of nitrogen atom in bonding with titanium ion. The asymmetric and symmetric CO_2 stretching vibrations appeared at 1602 cm^{-1}, 1346 cm^{-1}, respectively in the complex with the difference of 256 cm^{-1} in wavenumber suggesting the involvement of unidentate carboxylate group in coordination with titanium ion. The shift in wavenumber of peaks due to C–O (phenolic) and COO^- (C–O) stretching vibrations appearing at 1144 and 1255 cm^{-1} compared to salicylic acid (1151, 1291 cm^{-1}, respectively) confirmed the coordination through oxygen atoms. In complex **4**, the vibrations at 1087 cm^{-1} and 1015 cm^{-1} corresponded to the terminal and bridged butoxy group. The appearance of a new band at 423 cm^{-1} was assigned to ν_{Ti-N} (L^{IV}). Two new bands at 530 cm^{-1} and 559 cm^{-1}, respectively established the formation of Ti–O (ν_{Ti-O}) bond due to coordination of titanium with salicylate ion(sal).

In case of complex **5**, the N–H peak of indole moiety appeared at 3203 cm^{-1} with broadening and shift towards lower wavenumber indicating the involvement of nitrogen atom in coordination with titanium ion. The two CO_2 vibrations (asymmetric and symmetric) appeared at 1601 cm^{-1}, 1348 cm^{-1} with $\Delta\nu$ = 253 cm^{-1} described the participation of unidentate carboxylate group in bonding with a metal ion. The peaks due to C–O (phenolic) and COO^- (C–O) stretching vibrations appeared at 1145 cm^{-1} and 1246 cm^{-1} wavenumber with lowering of 6–45 cm^{-1} as compare to salicylic acid (1151, 1291 cm^{-1}, respectively) confirmed bonding through oxygen atoms. The peak due to OH bending vibration was missing in the complex. Peaks due to the terminal and bridged butoxy group in complex appeared at 1101 cm^{-1}, 1034 cm^{-1}, respectively. The new peak due to ν_{Ti-N} (L^V) stretching mode appeared at 420 cm^{-1} while peak due to ν_{Ti-O} (sal) observed at 532 cm^{-1}, 535 cm^{-1}.

3.2 *^{1}H-NMR spectra*

The complexation of titanium metal with ligands (H_2sal, L^{I-V}) was confirmed by proton NMR spectroscopic technique. The ^{1}H-NMR of all complexes (**1–5**) showed two types of butoxy groups peaks (Table T2, Supplementary Information). The peaks corresponding to the carboxylic and phenolic hydrogens of salicylic acid at 13.44 and 11.52 ppm disappeared in all complexes, thereby indicated carboxylate and phenolate formation.[25]

Evaluation of ^{1}H-NMR of all complexes had peaks of two types of butoxy groups in two different coordination mode i.e., terminal and bridged. Complex **1** showed terminal butoxy groups between 0.87 ppm (CH_3 protons), 1.28–1.39 ppm (CH_2 protons) and 3.42 ppm (OCH_2 protons). The bridged butoxy group peaks were found at 1.37–1.41 ppm (CH_2 protons), 0.93 ppm (CH_3 protons), and 4.32 ppm (OCH_2 protons). The presence of two types of peaks for each set of protons suggested that butoxy group had both terminal and bridged coordination mode.[23] The aromatic protons were reported in the range of 6.94–7.95 ppm. The N–H proton of complex **1** exhibited peak at 8.19 ppm with a downfield shift of 0.14 ppm suggested the participation of lone pair of electron on nitrogen atom in bonding with titanium ion. The OH group was found at 3.87 ppm with a very slight shift from pure ligand (L^I) (3.89 ppm). Complex **2** due to solubility problem didn't exhibit clear proton NMR spectrum. However, the terminal and bridged butoxy protons were found in the range 0.86 ppm (CH_3 protons), 1.23–1.38 ppm (CH_2 protons), 3.18 ppm (OCH_2 protons) and 0.95 ppm (CH_3 protons), 1.36–1.42 ppm (CH_2 protons), 4.30 ppm (OCH_2 protons), respectively. The N–H proton presented at 10.42 with a large downfield shift of 2.40 ppm thereby suggested the involvement of lone pair on the nitrogen atom in bonding with titanium metal. The aromatic protons were found at 6.58–7.74 ppm in the spectrum. The OCH_3 protons were observed with almost no shift in position at 3.88 ppm.[26] Complex **3** displayed the peaks of terminal butoxy group at 0.84 ppm (CH_3 protons), 1.20–1.36 ppm (CH_2 protons) and 3.35 ppm (OCH_2 protons). The bridged butoxy group had peaks at 0.88 ppm (CH_3 protons), 1.35–1.45 ppm (CH_2 protons) and 4.25 ppm (OCH_2 protons). The peak around

Table 2. Mass spectral analysis of titanium complexes

Titanium complexes	Major common peaks (m/z)
$[Ti(sal)L^{I-V}(OBu)(\mu\text{-}OBu)]_2$ (**1–5**)	136.99 $[C_7H_5O_3]^+$, 178.93$[C_7H_6O_3 + K]^+$, 241.86 $[TiC_{10}H_{10}O_4]^+$, 256.94 $[TiC_{11}H_{13}O_4]^+$, 402.86 $[TiC_{19}H_{31}O_6]^+$ and 512.48 $[Ti_2C_{22}H_{26}O_8]^+$

11.13 ppm corresponded to C–H (aldehyde of indole moiety) found with the downfield shift of 1.10 ppm. The N–H peak of pure ligand (L^{III}) shifted downfield from 8.97 ppm to 9.70 ppm indicated the participation of nitrogen atom in bonding with titanium ion. The aromatic protons appeared as a broad peak between 6.63–7.90 ppm. Complex **4** displayed a large downfield shift in the N–H peak of indole nucleus at 10.59 ppm from 8.63 ppm in pure ligand thus suggested the participation of nitrogen in coordination with a metal ion. The aromatic protons were observed in the region 6.59–7.81 ppm. The terminal butoxide group signals were found between 0.85 ppm (CH_3 protons), 1.30–1.39 ppm (CH_2 protons) and 3.35 ppm (OCH_2 protons). The bridged butoxide group showed peaks in the proton NMR spectra at 0.94 ppm (CH_3 protons), 1.38–1.42 ppm (CH_2 protons) and 4.35 ppm (OCH_2 protons). Complex **5** exhibited terminal and bridged butoxy protons at 0.86 ppm, 0.98 ppm (CH_3 protons), 1.14–1.35, 1.34–1.44 ppm (CH_2 protons) and 3.34, 4.38 ppm (OCH_2 protons) respectively. The N–H peak of indole moiety was at 10.78 ppm while aromatic protons were found in the region 6.55–7.79 ppm in the spectrum. The peaks found in all the spectra at about 2.50 ppm and 3.34 ppm corresponded to solvent peaks due to DMSO and tetrahydrofuran, respectively. The NMR spectra support the formation of dimeric structure on the basis of literature.[27]

3.3 *Mass spectra*

The formation of complexes (**1–5**) further established by recording their mass spectra. ESI-mass spectra of all complexes displayed some common fragmentation peaks (Table 2). The peak at m/z = 136.99 in all complexes was due to the presence of $[C_7H_5O_3]^+$ fragment (salicylic acid – H^+). Other common peaks were observed in all complexes at m/z = 178.93, 241.86, 256.95, 402.86 and 512.48 due to $[C_7H_6O_3 + K]^+$, $[TiC_{10}H_{10}O_4]^+$, $[TiC_{11}H_{13}O_4]^+$, $[TiC_{19}H_{31}O_6]^+$ and $[Ti_2C_{22}H_{26}O_8]^+$ fragments, respectively. The molecular ion peaks at m/z = 981.48, 950 were found for complexes **1** and **3**, respectively of very low intensity. These peaks corresponded to the dimeric structure of titanium complexes. Figure 1 describes the major common fragments of different complexes.

The results of all characterizations (FTIR, proton NMR, Mass spectrometry), indicated the involvement of (1) two types of butoxy groups (terminal and bridged), (2) carbonyl oxygen and phenolic oxygen with titanium metal center and (3) dimeric structure of

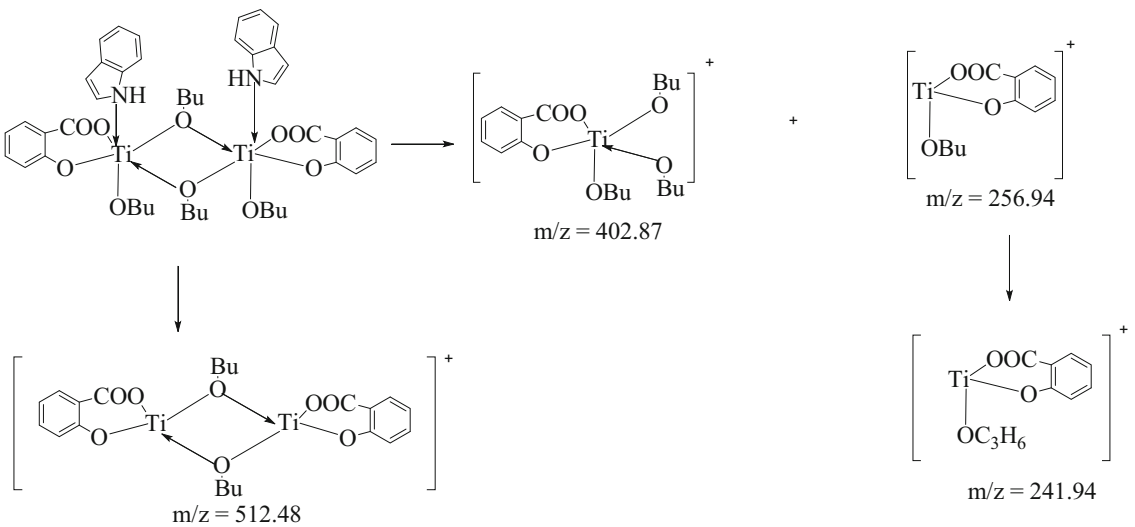

Figure 1. Common fragments of complexes $[Ti(sal)L^{I-V}(OBu)(\mu\text{-}OBu)]_2$ (1–5).

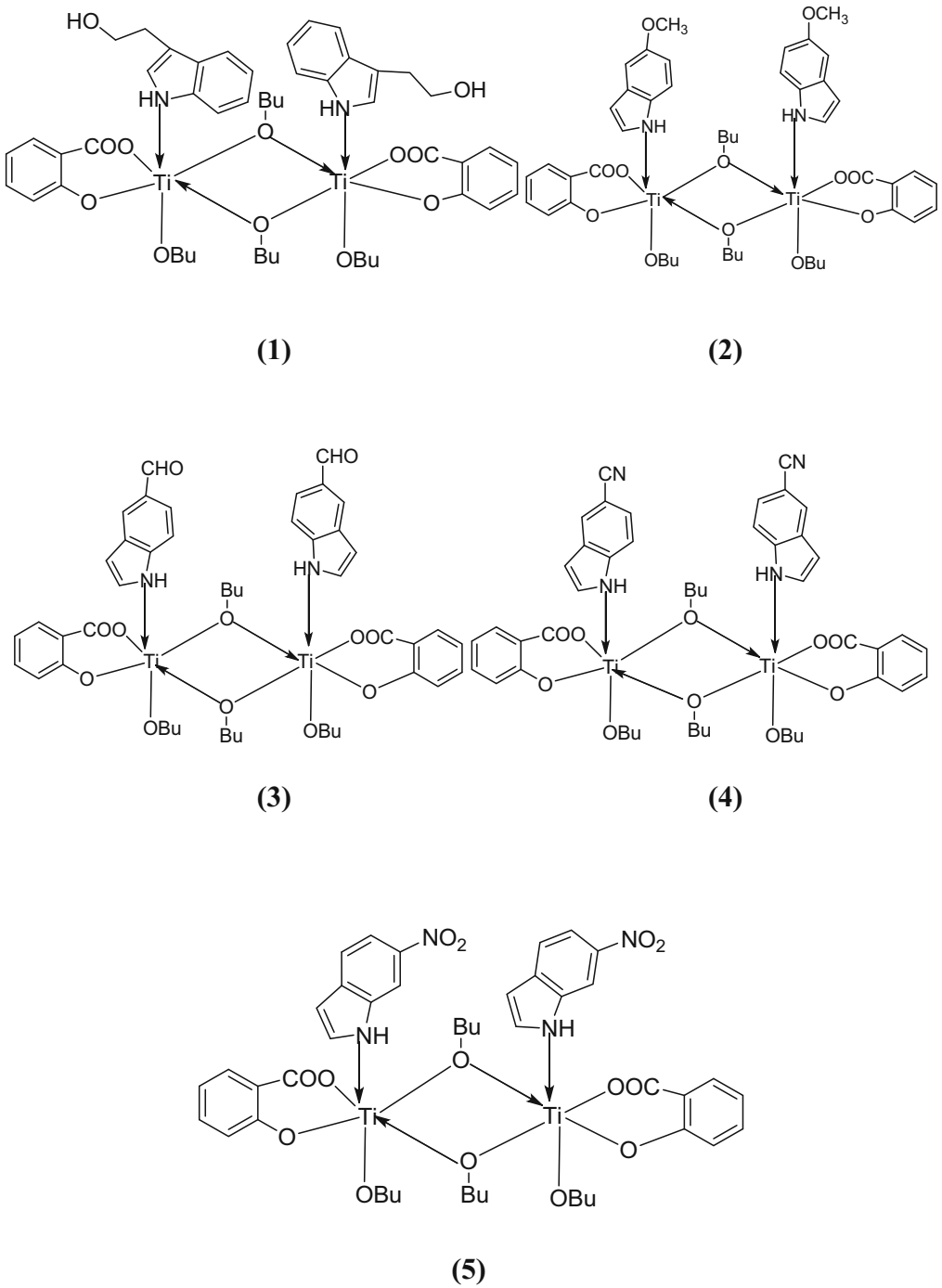

Figure 2. Proposed structure of $[Ti(sal)L^{I–V}(OBu)(\mu\text{-}OBu)]_2$ complexes (1–5).

all complexes **1–5**. Based upon the above information, the proposed structure of titanium complexes (**1–5**) has been shown in Figure 2.

3.4 *Biological studies*

3.4a *DNA-binding study*: The electronic absorption titration experiment was performed to investigate the binding affinity of titanium complexes with ct-DNA. General spectral characteristics of electronic titrations of complexes with ct-DNA involve hyperchromism and hypochromism. Hyperchromism emerges from the cleavage of secondary DNA structure while hypochromism incorporated with intercalative DNA binding between DNA base pairs and aromatic chromophores of complexes.[28] The electronic absorption spectra of titanium complexes (**1–5**) in the absence and presence of the incremental amount of ct-DNA were shown in Figures 3–7. Addition of increasing amount

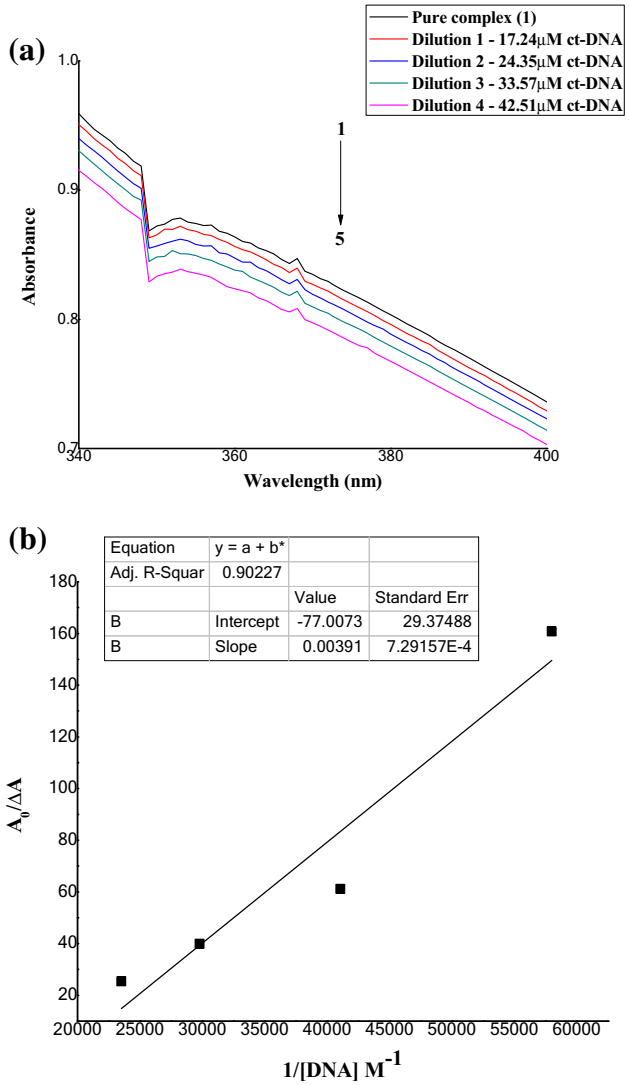

Figure 3. (**a**) Absorption spectra of complex [Ti(sal)L^{I}(-OBu)(μ-OBu)]$_2$ (**1**); in the absence and presence of an increasing concentration of ct-DNA. [Complex] = 20 μM, [DNA] = 0–42 μM. Arrow indicates the change in absorbance upon the incremental amount of DNA. (**b**) Plot of A_o/ΔA vs. 1/[DNA] for the titration of ct-DNA with complex **1**.

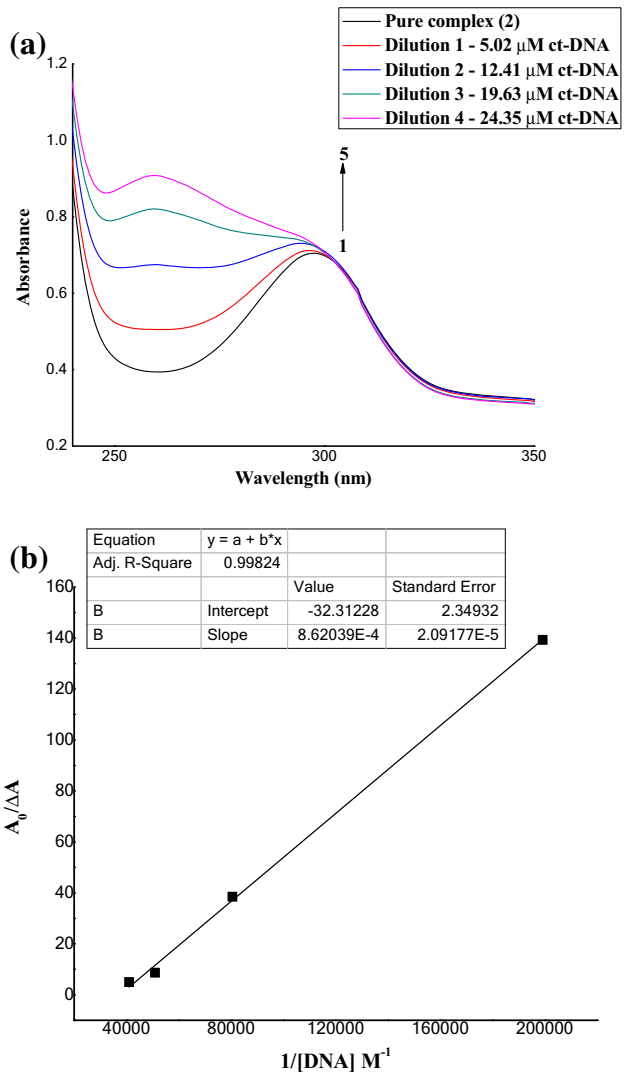

Figure 4. (**a**) Absorption spectra of complex [Ti(sal)L^{II}(-OBu)(μ-OBu)]$_2$ (**2**); in the absence and presence of an increasing concentration of ct-DNA. [Complex] = 20 μM, [DNA] = 0–24 μM. Arrow indicates the change in absorbance upon the incremental amount of DNA. (**b**) Plot of A_o/ΔA vs. 1/[DNA] for the titration of ct-DNA with complex **2**.

of ct-DNA to a fixed concentration of complexes (**1** and **4**) showed hypochromism which is generally related to the strength of DNA interaction.[29] The observed increase in hypochromism followed the order complex **1**) > complex **4**. Benesi-Hildebrand equation was used to examine the binding constant (K_b) which showed the binding strength of complexes.

$$\frac{A_0}{A - A_0} = \frac{\varepsilon_G}{\varepsilon_{H-G} - \varepsilon_G} + \left(\frac{\varepsilon_G}{\varepsilon_{H-G} - \varepsilon_G}\right) \times \frac{1}{K[DNA]}$$

The plots of A_o/ΔA vs. 1/[DNA] was prepared and the ratio of intercept to slope gave the value of binding constant. Complex **2**, **3** and **5** displayed hyperchromism with blue shift. These inspections are characteristic features of non-intercalative probably groove/electrostatic DNA-binding modes leading to slight perturbations. These complexes might have positive-charged metal moiety which expected to directly affect DNA.[30] These charged moieties can bind to glycoproteins, membrane proteins or cellular proteins. These observed spectral changes might be due to classical electrostatic interactions of charged moiety with negatively charged oxygen of phosphate group of DNA. Besides these effects, other electrostatic interactions like hydrogen bonding between the

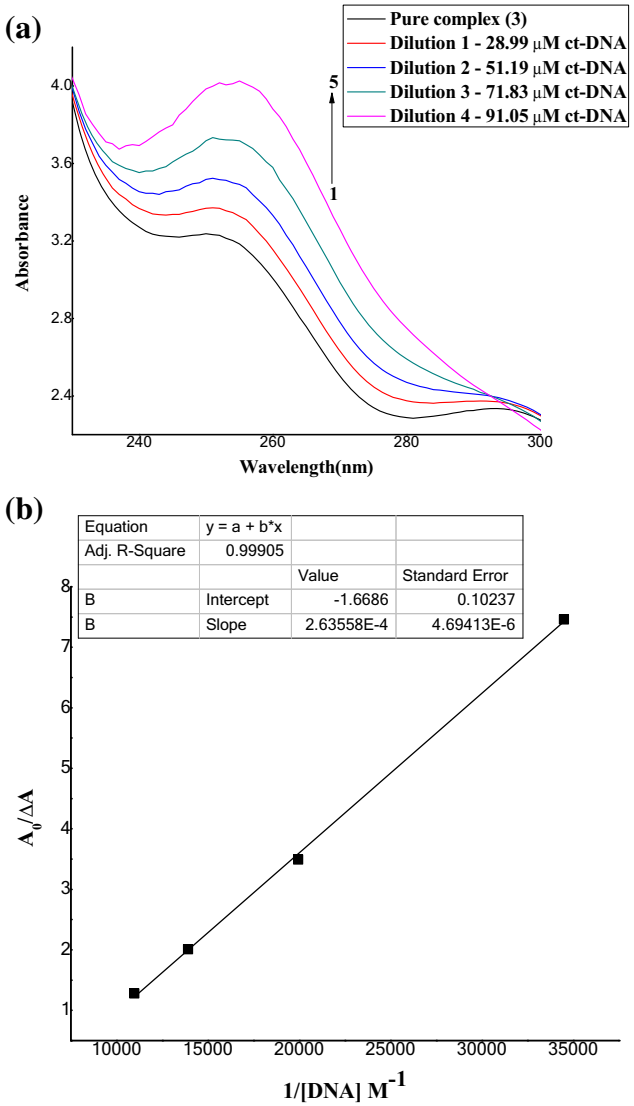

Figure 5. (**a**) Absorption spectra of complex [Ti(sal)L^{III}(-OBu)(μ-OBu)]$_2$ (**3**); in the absence and presence of increasing concentration of ct-DNA. [Complex] = 20 μM, [DNA] = 0–91 μM. Arrow indicates the change in absorbance upon the incremental amount of DNA. (**b**) Plot of A_o/ΔA vs. 1/[DNA] for the titration of ct-DNA with complex **3**.

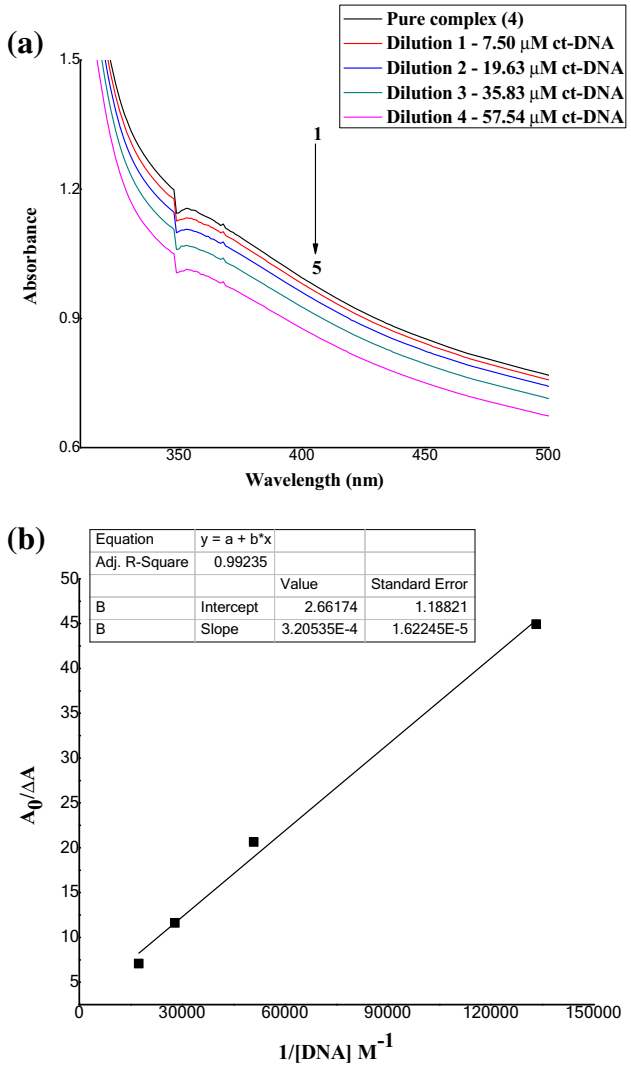

Figure 6. (**a**) Absorption spectra of complex [Ti(sal)L^{IV}(-OBu)(μ-OBu)$_2$] (**4**); in the absence and presence of an increasing concentration of ct-DNA. [Complex] = 20 μM, [DNA] = 0–57 μM. Arrow indicates the change in absorbance upon the incremental amount of DNA. (**b**) Plot of A_o/ΔA vs. 1/[DNA] for the titration of ct-DNA with complex **4.** (**a**) Absorption spectra of complex [Ti(sal)L^{V}(OBu)(μ-OBu)]$_2$ (**5**); in the absence and presence of an increasing concentration of ct-DNA. [Complex] = 20 μM, [DNA] = 0–96 μM. Arrow indicates the change in absorbance upon the incremental amount of DNA. (**b**) Plot of A_o/ΔA vs. 1/[DNA] for the titration of ct-DNA with complex **5**.

synthesized complexes and DNA base pairs may also present.[31]

To access the binding strength of titanium complexes (1–5), the binding constant was evaluated (Table 3). Complex **2** demonstrated highest binding constant (K_b = 37.48 × 10^3) among all complexes. Change in Gibbs free energy (ΔG) is an important parameter, which reflects the stability and binding degree of the formed adduct. ΔG can be calculated according to the following equation: ΔG = ΔH − TΔS. The negative values of ΔG (Table 3) indicated that the binding process is spontaneous and the stable complexes are formed between titanium complex and DNA.

3.4b *Fluorescence spectroscopy*: Fluorescence spectroscopy is a selective and sensitive technique used to investigate the binding mechanism of titanium complexes-DNA interactions.[32] The experiment was executed by the addition of a different increasing amount of ct-DNA to the fixed concentration of titanium complexes in the presence of Tris-HCl (5 mM) buffer solution containing NaCl (50 mM) at pH 7.2. The fluorescence spectra of titanium complexes (**1–5**) (Figures 8–12) upon excitation at 320 nm wavelength exhibited a major peak at 415 nm. On increasing the concentration of ct-DNA, the intensities of

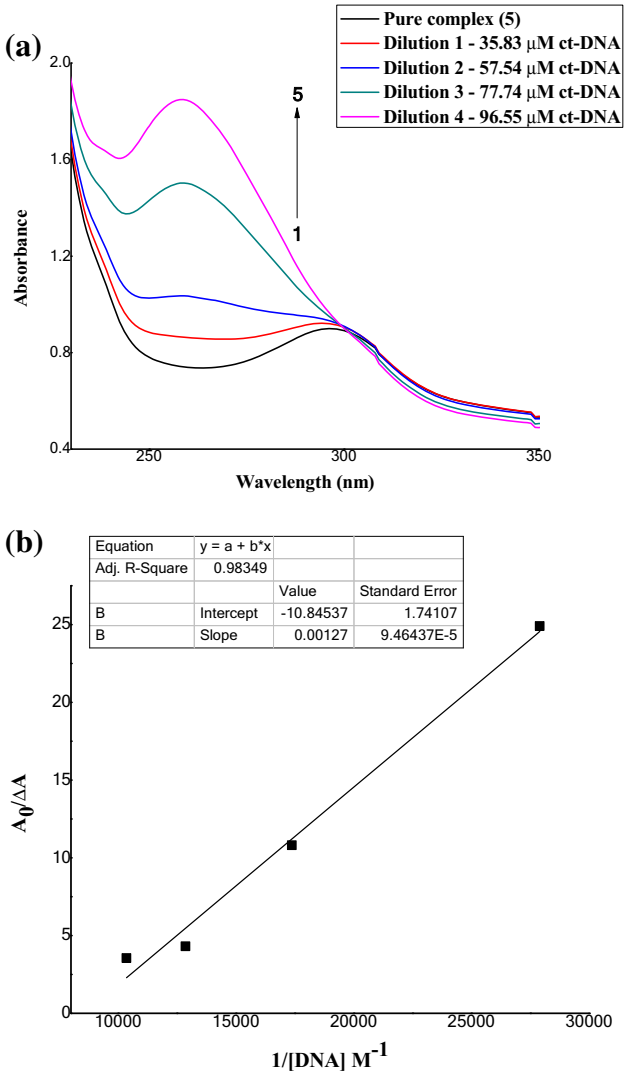

Figure 7. (**a**) Absorption spectra of complex [Ti(sal)L^{V}(-OBu)(μ-OBu)]$_2$ (**5**); in the absence and presence of an increasing concentration of ct-DNA. [Complex] = 20 μM, [DNA] = 0–96 M. Arrow indicates the change in absorbance upon the incremental amount of DNA. (**b**) Plot of $A_o/\Delta A$ vs. 1/[DNA] for the titration of ct-DNA with complex **5**.

[TiLL^{I-V}(OBu)(μ-OBu)]$_2$ increased regularly with no shift in wavelength. The result of an increase in fluorescence intensities of complexes indicated groove mode of binding with ct-DNA.[33, 34] Fluorescence technique was further used to determine binding constant (K_b) using the following equation.

$$\frac{1}{\Delta I} = \frac{1}{(K_b.\Delta I_0)[DNA]} + \frac{1}{\Delta I_0}$$

Table 4 displayed the values of binding constant which was calculated by the ratio of intercept to the slope of the plot 1/ΔI vs. 1/[DNA]. Complex **2** exhibited the highest binding constant (26.90×10^4 mol^{-1}). The results were similar as obtained from electronic absorption spectroscopy. The binding constants value found in the range (4.82×10^4–26.90×10^4 mol^{-1} for [Ti(sal)L^{I-V}(-OBu)(μ-OBu)]$_2$ (1–5) complexes.

3.4c *Antioxidant study*: Assessment of antioxidant activity for titanium complexes (1–5) was estimated in terms of reduction in absorbance of DPPH solution at 517 nm. This activity was produced by the ability of complex to release hydrogen and give rise to the reduced form of DPPH radical. The investigated changes in the free radical scavenging potential of the synthesized complexes and standard (ascorbic acid) on the basis of per cent inhibition were presented in Figure 13. Radical scavenging activity of titanium complexes as well as standard was increased in a dose-dependent manner.

All complexes had lower activity than the standard (ascorbic acid). Position, nature and electronic environment of substituents[35] had a prominent effect on the antioxidant activity as can be seen from results also.

3.4d *DNA cleavage activity*: The synthesized mixed ligand titanium butoxide complexes (1–5) were investigated for their DNA cleavage against ct-DNA using agarose gel electrophoresis method. Many anticancer drugs attacked DNA as their principal target.[36] Complexes having better DNA-binding ability have higher cleavage efficiency which helps in the designing of more effective DNA targeted drugs.[37] Figure 14 revealed that all complexes acted on ct-DNA by changing its supercoiled form (I) to open circular form (II). Cleavage efficiency of **4** and **5** were better than others due to their complete conversion of form I into form II which suggested them as the growth inhibitor of pathogenic organism by breaking the genome.[38] Also, the oxidative cleavage of DNA was checked by treating DNA alone with hydrogen peroxide where it completely changes the form (I) into form (II). These observations suggested that the synthesized complexes have the ability to split the DNA strands without the use of oxidizing agents.

3.4e *Antimicrobial activity*: In vitro antimicrobial screening of synthesized metal complexes involved their action against bacterial species P. aeruginosa (MTCC-3542), E. coli (MTCC-9721), L. monocytogenes (MTCC-675), S. flexneri (MTCC-1457), B. cereus (MTCC-1272), S. aureus (MTCC-11949) and fungal species B. cinerea, A. niger, P. expansum and A. alternate, respectively. The results of both antibacterial and antifungal studies were compared with their respective standards (tetracycline and fluconazole) in terms of zone of inhibition diameter (mm) (Tables T3 and T4, Supplementary Information). With respect to bacterial strains, only complexes **2** and **3** were found to be active antibacterial agents against S. aureus, L. monocytogenes and E. coli, S. aureus, L. monocytogenes, respectively.

Table 3. Binding constant and Gibb's free energy of titanium complexes $[Ti(sal)L^{I–V}(OBu)(\mu\text{-}OBu)]_2$ from electronic absorption spectra

Sl. no.	Compounds	Binding constant (K_b) (mol^{-1})	ΔG (K J mol^{-1})
1	$[Ti(sal)L^{I}(OBu)(\mu\text{-}OBu)]_2$ (**1**)	19.69×10^3	− 24.50
2	$[Ti(sal)L^{II}(OBu)(\mu\text{-}OBu)]_2$ (**2**)	37.48×10^3	− 26.12
3	$[Ti(sal)L^{III}(OBu)(\mu\text{-}OBu)]_2$ (**3**)	6.33×10^3	− 21.67
4	$[Ti(sal)L^{IV}(OBu)(\mu\text{-}OBu)]_2$ (**4**)	8.30×10^3	− 22.36
5	$[Ti(sal)L^{V}(OBu)(\mu\text{-}OBu)]_2$ (**1**)	8.54×10^3	− 22.42

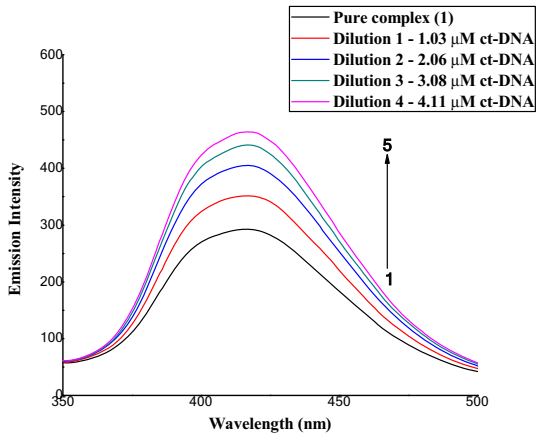

Figure 8. Fluorescence emission spectra of complex $[Ti(sal)L^{I}(OBu)(\mu\text{-}OBu)]_2$(**1**); in the absence and presence of an increasing concentration of ct-DNA. [DNA] = 0–4 μM. Arrow indicates the change in intensity upon the increase of DNA concentration.

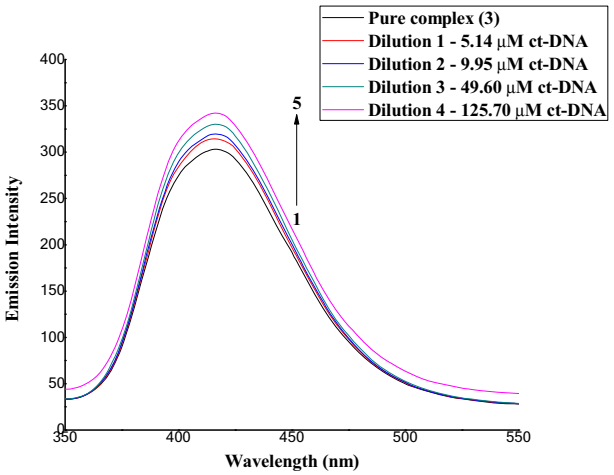

Figure 10. Fluorescence emission spectra of complex $[Ti(sal)L^{III}(OBu)(\mu\text{-}OBu)]_2$ (**3**); in the absence and presence of an increasing concentration of ct-DNA. [DNA] = 0–126 μM. Arrow indicates the change in intensity upon the increase of DNA concentration.

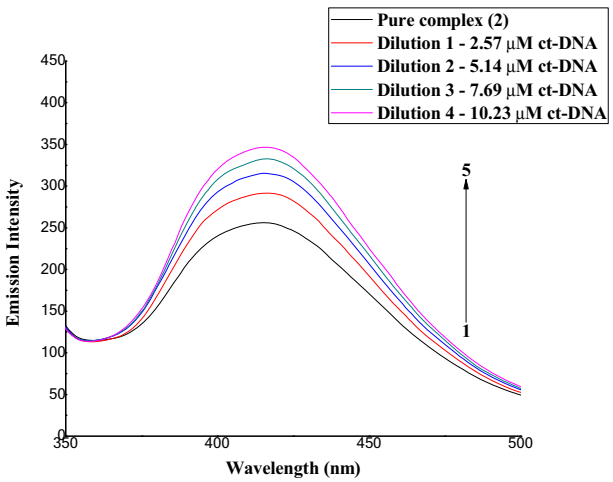

Figure 9. Fluorescence emission spectra of complex $[Ti(sal)L^{II}(OBu)(\mu\text{-}OBu)]_2$ (**2**); in the absence and presence of an increasing concentration of ct-DNA. [DNA] = 0–10 μM. Arrow indicates the change in intensity upon the increase of DNA concentration.

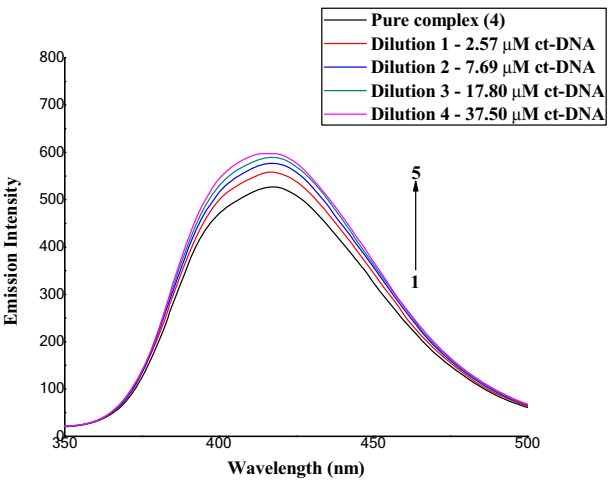

Figure 11. Fluorescence emission spectra of complex $[Ti(sal)L^{IV}(OBu)(\mu\text{-}OBu)]_2$ (**4**); in the absence and presence of increasing concentration of ct-DNA. [DNA] = 0–37 μM. Arrow indicates the change in intensity upon the increase of DNA concentration.

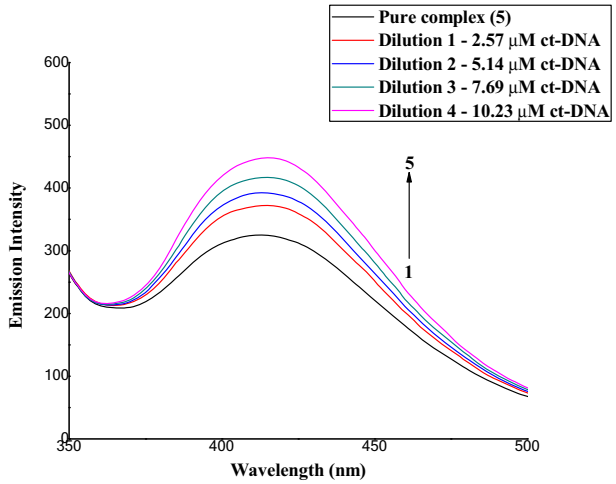

Figure 12. Fluorescence emission spectra of complex $[Ti(sal)L^{V}(OBu)(\mu\text{-}OBu)]_2$ (**5**); in the absence and presence of an increasing concentration of ct-DNA. [DNA] = 0–10 μM. Arrow indicates the change in intensity upon the increase of DNA concentration.

The results of antifungal activity revealed that complex **2**, **4**, **5** possessed more activity against *P. expansum*. The abnormality in the activity of different complexes against tested organisms depends on either the difference in ribosomes of microbial cells or impermeability of cells of the microbes.[39]

The effect of nature of ligand on the normal cell processes might be the reason for increased antimicrobial activity of complexes. An important factor that governs the antimicrobial activity of complexes against various organisms is liposolubility. It describes the passage of lipid-soluble material through lipid membrane that surrounds the cell.[40, 41] This enhanced lipophilicity blocks the binding sites of metal present in the enzymes by increasing the penetration of metal complexes into the lipid membranes. Further, the complexes showing antimicrobial activity obstruct the proteins synthesis which inhibits the growth of

Table 4. Binding constant of titanium complexes $[Ti(sal)L^{I–V}(OBu)(\mu\text{-}OBu)]_2$ from fluorescence spectra

Sl. no.	Compounds	Binding constant (K_b) (mol^{-1})
1	$[Ti(sal)L^{I}(OBu)(\mu\text{-}OBu)]_2$ (**1**)	10.12×10^4
2	$[Ti(sal)L^{II}(OBu)(\mu\text{-}OBu)]_2$ (**2**)	26.90×10^4
3	$[Ti(sal)L^{III}(OBu)(\mu\text{-}OBu)]_2$ (**3**)	4.82×10^4
4	$[Ti(sal)L^{IV}(OBu)(\mu\text{-}OBu)]_2$ (**4**)	7.92×10^4
5	$[Ti(sal)L^{V}(OBu)(\mu\text{-}OBu)]_2$ (**5**)	8.85×10^4

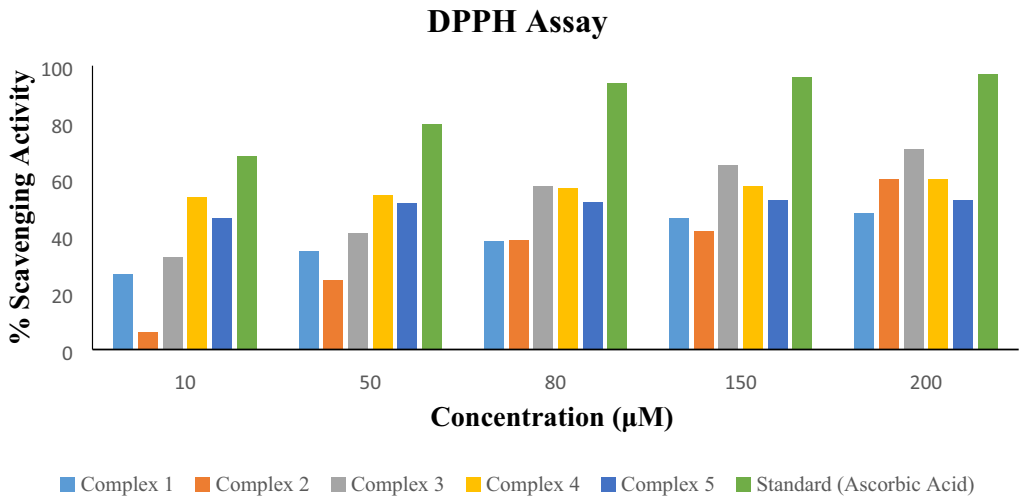

Figure 13. Bar graph representation of free radical scavenging activity (% inhibition) of titanium complexes $[Ti(sal)L^{I–V}(OBu)(\mu\text{-}OBu)]_2$ (1–5) against ascorbic acid (standard).

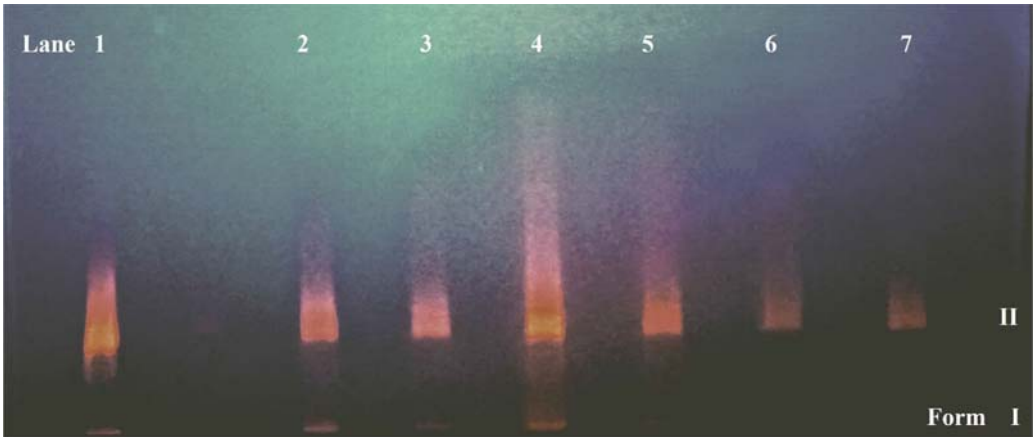

Figure 14. Gel electrophoresis of ct-DNA samples. Lane 1: DNA alone; Lane 2: DNA + complex 1; Lane 3: DNA + complex 2, Lane 4: DNA + complex 3, Lane 5: DNA + complex 4, Lane 6: DNA + complex 5; Lane 7: DNA + H_2O_2.

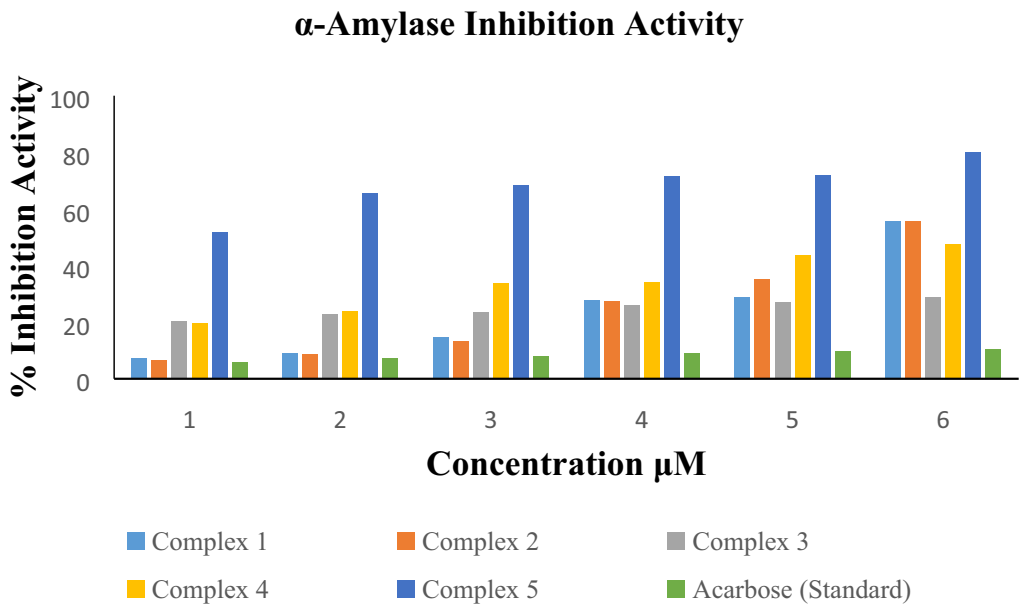

Figure 15. Bar graph of titanium complexes between % inhibition activity and concentration of complexes.

Table 5. Enzyme (α-amylase) inhibition activity by titanium $[Ti(sal)L^{I–V}(OBu)(\mu\text{-}OBu)]_2$ complexes (1–5)

Complexes	IC_{50} (µM)
$[Ti(sal)L^{I}(OBu)(\mu\text{-}OBu)]_2$ (**1**)	144.80
$[Ti(sal)L^{II}(OBu)(\mu\text{-}OBu)]_2$ (**2**)	138.35
$[Ti(sal)L^{III}(OBu)(\mu\text{-}OBu)]_2$ (**3**)	180.13
$[Ti(sal)L^{IV}(OBu)(\mu\text{-}OBu)]_2$ (**4**)	82.92
$[Ti(sal)L^{V}(OBu)(\mu\text{-}OBu)]_2$ (**5**)	8.02
Acarbose	552.75

microorganism by interrupting the respiration process of the cell.[42]

3.4f *Anticancer activity*: The efficacy of synthesized titanium complexes as anticancer agents against selected cell lines (L929 and L6) was checked using MTT assay. Supplementary Table T5 described the IC_{50} values of titanium complexes (1–5) against both cell lines. Analysis of result defined complexes **1** and **2** as a better cytotoxic agent than respective ligands against L6 cell line. In other cases, ligands performed better cytotoxicity against selected cell lines. All complexes were ineffective against L929 cell line

except complex **2** which showed low activity. In case of L6 cell line, complexes **1**, **2** displayed good activity while complex **4** showed low activity and complexes **3**, **5** had very low activity. Clearly, the steric hindrance in complexes along with the position and nature of substituent groups in indoles ($L^{I–V}$) affected the cytotoxic behaviour of complexes.

3.4g *α-Amylase inhibition study*: Alpha-amylase catalyzes the hydrolysis of glycosidic bonds (α-1,4-glycosidic bonds) present in different polysaccharides and starch lead to the formation of various small molecules of sugars such as glucose and maltose. When the formation of such sugar molecules exceeds the limit, it gives rise to diabetes. Therefore, in order to avoid postprandial hyperglycemia, the activity of α-amylase should be in control.[43] In an attempt to inhibit the α-amylase activity, we chose the titanium (IV) complexes with indole derivatives synthesized in our study. The different concentrations of these complexes were tested against α-amylase action. For comparison purpose, the same concentrations of standard drug (acarbose) have been taken. The results in terms of IC_{50} and inhibition activity exhibited by complexes were presented in Table T5 (Supplementary Information) and Figure 15, respectively. The observed inhibition activity of the complexes may be because of their binding to the oxygen atoms of the enzymes. The difference in activity of different complexes may be due to different salvation behaviour in action media. Therefore, complex **5** exhibited greater relevance than others in the development of new oral antidiabetic drug (Table 5).

4. Conclusions

In this paper, synthesis and characterization of the dinuclear titanium complexes i.e., $[Ti(sal)L^{I–V}(-OBu)(\mu\text{-}OBu)]_2$ with bidentate ligand (salicylic acid) and unidentate ligand (substituted indoles) were carried out. The results of spectroscopic characterization using FTIR technique confirmed the presence of unidentate carboxylate group in bonding with titanium ion. Both FTIR and proton NMR results confirmed the presence of phenolate, carboxylate groups and two types of butoxy groups i.e., terminal and bridged butoxy groups participating in bonding with metal centre. The appearance of a downfield shift of N–H peak of indole moiety in ^{1}H-NMR spectra of complexes suggested the participation of lone pair of electron of the nitrogen atom in coordination with titanium centre. All these findings pointed towards the formation of dimeric species which was further confirmed by mass spectrometry. Mode of binding of synthesized titanium complexes with ct-DNA was analyzed by using electronic absorption and fluorescence spectroscopy. DNA binding studies using UV-visible and fluorescence spectroscopy displayed groove/electrostatic binding in all complexes. Complexes (**1–5**) showed moderate to good antioxidant activity. DNA cleavage study using gel electrophoresis stated that complexes **4** and **5** had better efficacy to uncoil the strands of ct-DNA. Among synthesized complexes, only complexes **2** and **3** acted as effective antibacterial agents against bacterial strains *S. aureus* and *L. monocytogenes* while complex **2**, **4** and **5** behaved as good antifungal agents against fungal strain *P. expansum*. Cytotoxicity of synthesized complexes was evaluated using MTT assay against L6 skeletal muscle cell line and L929 cancer cell line. Results displayed that complexes **1** and **2** had better cytotoxicity than their respective ligands (substituted indoles). Complex **5** emerged as the best oral antidiabetic drug with respect to all complexes.

Supplementary Information (SI)

Figures S1–S15 and Tables T1–T5 are available at www.ias.ac.in/chemsci.

References

1. Fulton J R, Holland A W, Fox D J and Bergman R G 2002 Formation, reactivity, and properties of nondative late transition metal-oxygen and -nitrogen bonds *Acc. Chem. Res.* **35** 44
2. Wolczanski P T 2009 Structure and reactivity studies of transition metals ligated by ^{t}BuSi$_3$X (X = O, NH, N, S, and CC) *Chem. Commun.* **7** 740
3. Buyuktas B S and Aktas O 2006 Complexation of titanium n-butoxide Ti(OBu^n)$_4$ and zirconium n-butoxide Zr(OBu^n)$_4$ with some oxime ligands and structural analysis of the complexes *Transit. Met. Chem.* **31** 56
4. Mehrotra R C 1990 Chemistry of alkoxide precursors *J. Non-Cryst Solids.* **121** 1
5. Sanchez C and Livage J 1990 Sol-gel chemistry of metal alkoxide precursor *New J. Chem.* **14** 513
6. Kaushik N K, Kaushik N, Attri P, Kumar N, Kim C H, Verma A K and Choi E H 2013 Biomedical importance of indoles *Molecules* **18** 6620
7. Dolle R E and Nelson K H Jr 1999 Comprehensive survey of combinatorial library synthesis *J. Comb. -Chem.* **1** 235
8. Franzén R G 2000 Recent advances in the preparation of heterocycles on solid support: a review of the literature *J. Comb. Chem.* **2** 195
9. Dolle R E 2001 Comprehensive survey of combinatorial library synthesis *J. Comb. Chem.* **3** 477
10. Chadha N and Silakari O 2017 Indoles as therapeutics of interest in medicinal chemistry: Bird's eye view *Eur. J. Med. Chem.* **134** 159
11. Raj K M and Mruthyunjayaswamy B H M 2017 Synthesis, spectroscopic characterization, electrochemistry and biological activity evaluation of some metal (II) complexes with ONO donor ligands containing

indole and coumarin moieties *J. Saudi Chem. Soc.* **21** S202
12. Kumar S, Pandya P, Pandav K, Gupta S and Chopra A 2012 Structural studies on ligand-DNA system. A rubst approach in drug design *J. Biosci*. **37** 553
13. Palchaudhuri R and Hergenrother P 2007 DNA as a target for anticancer compounds: Methods to determine the mode of binding and the mechanism of action *Curr. Opin. Biotechnol.* **18** 497
14. Mishra R, Kumar A, Chandra R and Kumar D 2017 A review on theoretical studies of various types of Drug-DNA interaction *IJSTS* **3** 11
15. Kaushal R, Thakur S and Nehra K 2016 ct-DNA Binding and Antibacterial Activity of Octahedral Titanium (IV) Heteroleptic (Benzoylacetone and Hydroxamic Acids) Complexes *Int. J. Med. Chem.* **2016** 1
16. Tabassam N, Ali S, Shahzadi S, Shahid M, Abbas M, Khan Q M, Sharma S K and Qanungo K 2013 Synthesis, characterziation, semi-empirical quantum-mechanical study and biological activity of organotin(IV) complexes with 2-ethylanilinocarbonylpropenoic acid *Russ. J. Gen. Chem.* **83** 2423
17. Kaushal R, Kumar N, Awasthi P and Nehra K 2013 Syntheses, characterization, and antibacterial study of titanium complexes *Turk. J. Chem.* **37** 936
18. Kaur V, Kumar M, Kumar A and Kaur S 2018 *Butea monosperma* (Lam.) Taub. Bark fractions protect against free radicals and induce apoptosis in MCF-7 breast cancer cells *via* cell-cycle arrest and ROS-mediated pathway *Drug Chem. Toxicol*. 1
19. Sudha P, Smita S Z, Shobha Y B and Ameeta R K 2011 Potent a-amylase inhibitory activity of Indian Ayurvedic medicinal plants *BMC Complement Altern. Med.* **11** 1
20. Trivedi M K, Branton A, Trivedi D, Shettigar H, Bairwa K and Jana S 2015 Fourier Transform Infrared and Ultraviolet-Visible Spectroscopic Characterization of Biofield Treated Salicylic Acid and Sparfloxacin *Nat. Prod. Chem. Res.* **3** 1
21. Mehrotra R C and Bohra R 1983 *Metal Carboxylates* (London UK: Academic Press)
22. Colthup N B, Daly L H and Wiberley S E 1990 *Introduction to Infrared and Raman Spectroscopy* 3rd edn. (Boston USA: Academic Press)
23. Ambreen S, Gupta K, Singh S, Gupta D K, Daniele S, Pandey N D and Pandey A 2013 Synthesis and structural characterization of some titanium butoxides modified with chloroacetic acids *Transit. Met. Chem.* **38** 835
24. Lawal A, Shodeinde A S, Amolegbe S A, Elaigwu S E and Yunus-Issa M T 2017 Synthesis, Characterization and Antimicrobial Activity of Mixed Transition Metal Complexes of Salicylic Acid with 1, 10-Phenanthroline *J. Appl. Sci. Environ. Manage.* **21** 568
25. Takač M J-M and Topić D V 2004 FT-IR and NMR spectroscopic studies of salicylic acid derivatives. II. Comparison of 2-hydroxy- and 2,4- and 2,5-dihydroxy derivatives *Acta Pharm.* **54** 177
26. Meng X, Wang X, Duan H, Bu J, Qin D and Zhang Y 2012 Design, synthesis, and characterization of indole derivatives *Res. Chem. Intermed.* **39** 3829
27. Mandal D, Chakraborty D, Ramkumar V and Chand D K 2016 Group 4 Alkoxide Complexes containing [NNO]-type Scaffold: Synthesis, Structural Characterization and Polymerization Studies *RSC Adv.* **6** 21706
28. Tan L F, Liu X H, Chao H and Ji L 2007 Synthesis, DNA-binding and photocleavage studies of ruthenium(II) complex with 2-(30-phenoxyphenyl)imidazo[4,5-f][1,10]phenanthroline *J. Inorg. Biochem.* **101** 56
29. Lakshmipraba J, Arunachalam S, Solomon R V, Venuvanalingam P, Riyasdeen A, Dhivya R and Akbarsha M A 2014 Surfactant-copper(II) Schiff base complexes: synthesis, structural investigation, DNA interaction, docking studies, and cytotoxic activity *J. Biomol. Struct. Dyn*. **33** 877
30. Falcioni M L, Pellei M and Gabbianelli R 2008 Interaction of tributyltin(IV) chloride and a related complex $[Bu_3Sn(LSM)]$ with rat leukocytes and erythrocytes: Effect on DNA and on plasma membrane *Mutat. Res.* **653** 57
31. Liu J, Zhang T, Lu T, Qu L, Zhou H, Zhang Q and Ji L 2002 D NA-binding and cleavage studies of macrocyclic copper(II) complexes *J. Inorg. Biochem.* **91** 269
32. Kundu P and Chattopadhyay N 2017 Interaction of a bioactive pyrazole derivative with calf thymus DNA: Deciphering the mode of binding by multi-spectroscopic and molecular docking investigations *J. Photochem. Photobiol. B Biol*. **173** 485
33. Chaurasia M, Tomar D and Chandra S 2019 Synthesis, spectroscopic characterization and DNA binding studies of Cu(II) complex of Schiff base containing benzothiazolemoiety *J. Taibah. Univ. Sci*. **13** 1050
34. Yang C-Z, Liang C-Y, Zhang D and Hu Y-J 2017 Deciphering the interaction of methotrexate with DNA: Spectroscopic and molecular docking study *J. Mol. Liq.* **248** 1
35. Shaikh Z, Ashiq U, Jamal R A, Mahroof-Tahir M, Shamshad B and Sultan S 2015 Chemistry and antioxidant properties of titanium(IV) complexes *Transit. Met. Chem.* **40** 665
36. Waring M 1977 *Structural and conformational studies on quinoxaline antibiotics in relation to the molecular basis of their interaction with DNA* In Drug Action at the Molecular Level (London: Palgrave Macmillan) pp. 167–189
37. Pyle A M, Rehmann J P, Meshoyrer R, Kumar C V, Turro N J and Barton J K 1989 Mixed-ligand complexes of Ruthenium (II): factors governing binding to DNA *J. Am. Chem. Soc*. **111** 3051
38. Kulkarni A, Patil S A and Badami P S 2009 Synthesis, characterization, DNA cleavage and in vitro antimicrobial studies of La(III), Th(IV) and VO(IV) complexes with Schiff bases of coumarin derivatives *Eur. J. Med. Chem.* **44** 2904
39. Prashanthi Y, Kiranmai K, Ira, K S K, Chityala V K and Shivaraj 2012 Spectroscopic Characterization and Biological Activity of Mixed Ligand Complexes of Ni(II) with 1,10-Phenanthroline and Heterocyclic Schiff Bases *Bioinorg. Chem. Appl.* **2012** 1
40. Raman N, Pothiraj K and Baskaran T 2011 DNA-binding, oxidative DNA cleavage, and coordination mode of later 3d transition metal complexes of a Schiff

base derived from isatin as antimicrobial agents *J. Coord. Chem*. **64** 3900
41. Jelokhani-Niaraki M, Kondejewski L H, Wheaton L C and Hodges R S 2009 Effect of Ring Size on Conformation and Biological Activity of Cyclic Cationic Antimicrobial Peptides *J. Med. Chem.* **52** 2090
42. Nejo A A, Kolawole G A and Nejo A O 2010 Synthesis, characterization, antibacterial, and thermal studies of unsymmetrical Schiff-base complexes of cobalt(II) *J. Coord. Chem*. **63** 4398
43. Philip J E, Shahid M, Kurup M R P and Velayudhan M P 2017 Metal based biologically active compounds: Design, synthesis, DNA binding and antidiabetic activity of 6-methyl-3-formyl chromone derived hydrazones and their metal (II) complexes *J. Photochem. Photobiol. B Biol*. **175** 178